Use this paper

ELSEVIER

Thin Solid Films 418 (2002) 182–188

thin solid films

www.elsevier.com/locate/tsf

Hsueh

Paper Verification Test in MATLAB conforms results in this paper

Thermal stresses in elastic multilayer systems

C.H. Hsueh*

Metals and Ceramics Division, Oak Ridge National Laboratory, Oak Ridge, TN 37831, USA

Received 6 December 2001; received in revised form 13 July 2002; accepted 30 July 2002

Abstract

Thermal stresses in elastic multilayer systems have been previously modelled. However, because the displacement compatibility condition at interfaces between layers must be satisfied, the complexity in obtaining a closed-form solution increases with the number of layers in the system. As a result, existing analyses often adopt simplifications (e.g. assuming a constant elastic modulus throughout the system) to obtain closed-form solutions or are solved numerically by computer. The present study develops an analytical model, in which the complexity in obtaining a closed-form solution is independent of the number of layers and an exact closed-form solution can be concisely formulated. Specific results are calculated for elastic thermal stresses in (AlGa)As laser diodes, which consist of five layers. Also, the zero-order and the first-order approximations are formulated based on the exact closed-form solution, and their accuracy is examined. The acceptability of assuming a constant elastic modulus in the system in existing analyses is also discussed.

Keywords: Multilayers; Stress; Elastic properties; Gallium arsenide

1. Introduction

Advanced systems of multiple film layers on substrates have been used extensively in microelectronic, optical, and structural components, and protective coatings [1]. The functionality and reliability of multilayered systems are strongly influenced by residual stresses. These stresses arise because of: (i) the thermal mismatch between the films and the substrate when the system is cooled from its fabrication temperature to room temperature; and (ii) growth stresses [2,3]. Considerable efforts have been devoted to the analysis of residual stresses in elastic multilayer systems [4–9]. The analyses are generally based on classical beam bending theory, and strain continuity at interfaces between layers is required. As a result, both the number of unknowns to be solved for and the number of continuity conditions to be satisfied increase with the number of layers in the system [4–9]. In such cases, obtaining a closed-form solution is a formidable task, and the analysis is either left to the computer [6,8] or simplified by assuming a constant elastic modulus throughout the system to obtain an approximate closed-form solution [4,5,8].

In analysing thermal stresses in bilayer systems, Hsueh and Evans found that a general equation could be used to describe the strain distribution in the system [10]. This was achieved by decomposing the total strain into a uniform strain component and a bending strain component. In this case, the strain continuity condition is automatically satisfied. The advantage of the above analysis is not obvious for bilayer systems because both this analysis and other analyses based on classical beam bending theory [11] contain three unknowns and three boundary conditions. However, the advantage of Hsueh and Evans' analysis becomes obvious for multilayer systems because there are still only three unknowns to be solved and three boundary conditions to be satisfied.

The purpose of the present study is to analyse thermal stresses in elastic multilayer systems. First, a general closed-form solution is derived. Then, the first-order and the zero-order approximations are formulated based

*Corresponding author. Tel.: +1-865-576-6586; fax: +1-865-574-8445.

E-mail address: hsuehc@ornl.gov (C.H. Hsueh).

0040-6090/02/$ - see front matter
PII: S0040-6090(02)00699-5

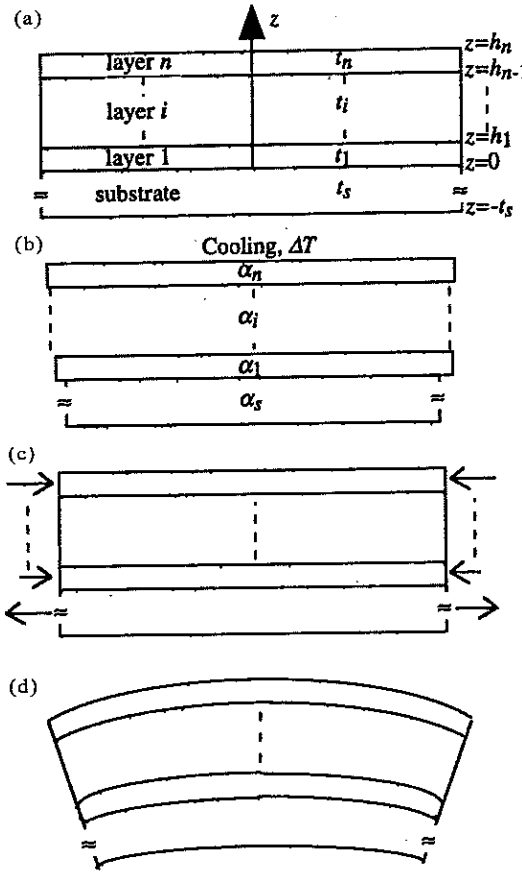

Fig. 1. Schematics showing bending of a multilayer strip due to thermal stresses: (a) stress-free condition; (b) unconstrained strains, $\varepsilon_i=\alpha_i\Delta T$ and $\varepsilon_s=\alpha_s\Delta T$, due to a temperature change, ΔT; (c) constrained strain, $\varepsilon_i=\varepsilon_s=c$, to maintain displacement compatibility; and (d) bending induced by asymmetric stresses.

on the exact closed-form solution. Finally, specific results are calculated for (AlGa)As laser diodes, which consist of five layers. The accuracy of the first-order and the zero-order approximations is addressed, and the acceptability of assuming a constant elastic modulus in the system in existing analyses is discussed.

2. Analyses

An elastic multilayered strip is shown schematically in Fig. 1a, where n layers of film with individual thicknesses, t_i, are bonded sequentially to a substrate with a thickness, t_s, at elevated temperatures. The subscript, i, denotes the layer number for the film and ranges from 1 to n with layer 1 being the layer in direct contact with the substrate. The coordinate system is defined such that the interface between the substrate and layer 1 of the film is located at $z=0$, the substrate's free surface is located at $z=-t_s$, the free surface of the outer-most film layer is located at $z=h_n$, and the interface between layers i and $i+1$ is located at h_i. With these definitions, the relation between h_i and t_i is described by

$$h_i=\sum_{j=1}^{i} t_j \ (i=1 \text{ to } n) \tag{1}$$

The multilayer system is cooled to room temperature, and the coefficients of thermal expansion (CTEs) of the substrate and the films are α_s and α_i, respectively. To determine the stress distribution in the system, the logic described by Hsueh and Evans [10] is used. First, the system experiences an unconstrained differential shrinkage due to the cooling temperature range, ΔT, such that thermal strains, $\alpha_s\Delta T$ and $\alpha_i\Delta T$, exist in the substrate and films, respectively (Fig. 1b). Uniform tensile/compressive stresses are then imposed on the individual layers to achieve displacement compatibility, such that the strain in the system is a constant, c, and the net force on the system remains zero (Fig. 1c). Finally, bending of the system occurs because of the asymmetric stresses in the system (Fig. 1d).

Based on the logic described in Fig. 1, the strain in the multilayer, ε, can be decomposed into a uniform component and a bending component. While the uniform strain component, c, is dictated by the logic in Fig. 1c, the bending component results from the logic described by Fig. 1d. Defining the bending axis as the line in the cross-section of the system where the bending strain component is zero, the bending strain component is proportional to the distance from the bending axis and inversely proportional to the radius of curvature. Hence, the total strain in the system can be formulated as [10]

$$\varepsilon=c+\frac{z-t_b}{r} \ (\text{for } -t_s\le z\le h_n) \tag{2}$$

where $z=t_b$ dictates the location of the bending axis, and r is the radius of curvature of the system. It should be noted that the bending axis defined in this work is different from the conventional neutral axis, which has been defined in classical beam bending theory as the line in the cross-section of the system where the normal stress is zero [12]. It should also be noted that by using Eq. (2) to describe the strain in the system, the strain continuity conditions at the interfaces between layers are automatically satisfied.

The normal stresses in the substrate and the films, σ_s and σ_i, are related to strains by

$$\sigma_s=E_s(\varepsilon-\alpha_s\Delta T) \ (\text{for } -t_s\le z\le 0) \tag{3}$$

$$\sigma_i=E_i(\varepsilon-\alpha_i\Delta T) \ (\text{for } i=1 \text{ to } n) \tag{4}$$

where E is Young's modulus, and the subscripts s and i denote the substrate and layer i of the film, respectively. If the system has a planar geometry rather than a strip, E should be replaced by the biaxial modulus, $E/(1-\nu)$, where ν is Poisson's ratio. Also, in the presence of growth stresses, the corresponding lattice mismatch

strain between layers should be superposed on the thermal strain.

The strain/stress distributions in multilayer systems are contingent upon solutions of the three parameters, c, t_b and r, which can be determined sequentially from the following three boundary conditions. First, the resultant force due to the uniform strain component (i.e. the total force in Fig. 1c) is zero:

$$E_s(c-\alpha_s\Delta T)t_s+\sum_{i=1}^{n}E_i(c-\alpha_i\Delta T)t_i=0 \tag{5}$$

The uniform strain component, c, can be determined from Eq. (5), such that

$$c=\frac{\left(E_st_s\alpha_s+\sum_{i=1}^{n}E_it_i\alpha_i\right)\Delta T}{E_st_s+\sum_{i=1}^{n}E_it_i} \tag{6}$$

Second, the resultant force due to the bending strain component is zero; i.e.

$$\int_{-t_s}^{0}\frac{E_s(z-t_b)}{r}dz+\sum_{i=1}^{n}\int_{h_{i-1}}^{h_i}\frac{E_i(z-t_b)}{r}dz=0 \tag{7}$$

The position of the bending axis can be determined from Eq. (7), such that

$$t_b=\frac{-E_st_s^2+\sum_{i=1}^{n}E_it_i(2h_{i-1}+t_i)}{2\left(E_st_s+\sum_{i=1}^{n}E_it_i\right)} \tag{8}$$

It should be noted that when $i=1$, h_{i-1} (i.e. h_0) is defined as zero. Third, the sum of the bending moment with respect to the bending axis ($z=t_b$) is zero, such that

$$\int_{-t_s}^{0}\sigma_s(z-t_b)dz+\sum_{i=1}^{n}\int_{h_{i-1}}^{h_i}\sigma_i(z-t_b)dz=0 \tag{9}$$

The curvature, $1/r$, can be determined from Eqs. (2)–(4) and (9), such that

$$\frac{1}{r}=\frac{3\left[E_s(c-\alpha_s\Delta T)t_s^2-\sum_{i=1}^{n}E_it_i(c-\alpha_i\Delta T)(2h_{i-1}+t_i)\right]}{E_st_s^2(2t_s+3t_b)+\sum_{i=1}^{n}E_it_i[6h_{i-1}^2+6h_{i-1}t_i+2t_i^2-3t_b(2h_{i-1}+t_i)]} \tag{10}$$

where c and t_b are given by Eqs. (6) and (8). With the solutions of c, t_b and r, the general solutions for the strain/stress distributions in multilayer systems are complete.

The solutions given above are exact. When the thicknesses of the film layers are much less than the substrate thickness, the solutions can be simplified. Taking a first-order approximation (i.e. ignoring terms with orders of t_i higher than one), Eqs. (6), (8) and (10) become

$$c=\alpha_s\Delta T+\sum_{i=1}^{n}\frac{E_it_i(\alpha_i-\alpha_s)\Delta T}{E_st_s} \tag{11}$$

$$t_b=-\frac{t_s}{2}\left(1-\sum_{i=1}^{n}\frac{E_it_i}{E_st_s}\right) \tag{12}$$

$$\frac{1}{r}=6\sum_{i=1}^{n}\frac{E_it_i(\alpha_i-\alpha_s)\Delta T}{E_st_s^2} \tag{13}$$

The curvature, $1/r$, given by Eq. (13) can be decomposed into the individual contribution of the thermal mismatch between the substrate and each film layer, such that

$$\frac{1}{r}=\sum_{i=1}^{n}\frac{1}{r_i} \tag{14}$$

where the curvature component, $1/r$, is given by

$$\frac{1}{r_i}=\frac{6E_it_i(\alpha_i-\alpha_s)\Delta T}{E_st_s^2} \tag{15}$$

Hence, the resultant curvature of the system is a linear superposition of the bending effect induced by the thermal mismatch between the substrate and each individual film layer.

The approximate stress distributions in the system can be obtained based on the above approximation. For the first-order approximation, the stress distributions can be derived from Eqs. (2)–(4), (11)–(13), such that

$$\sigma_s=\frac{2}{t_s^2}\left(3z+2t_s-\frac{2}{E_s}\sum_{j=1}^{n}E_jt_j\right)\sum_{i=1}^{n}E_it_i(\alpha_i-\alpha_s)\Delta T \ (\text{for } -t_s\le z\le 0) \tag{16}$$

$$\sigma_i=E_i\left[\alpha_s-\alpha_i+4\sum_{j=1}^{n}\frac{E_jt_j(\alpha_j-\alpha_s)}{E_st_s}\right]\Delta T \ (\text{for } i=1 \text{ to } n) \tag{17}$$

Eqs. (16) and (17) are expressed in terms of the thermal mismatch. Alternatively, the thermal stresses can also be expressed in terms of the curvature of the system:

$$\sigma_s=\frac{E_s}{3r}(3z+2t_s)-\frac{2}{3r}\sum_{i=1}^{n}E_it_i \ (\text{for } -t_s\le z\le 0) \tag{18}$$

$$\sigma_i=-\frac{E_st_s^2}{6t_ir_i}+\frac{2E_it_s}{3r} \ (\text{for } i=1 \text{ to } n) \tag{19}$$

where r and r_i are given by Eqs. (13) and (15), respectively.

The above first-order approximation can further be simplified to obtained the zero-order approximation,

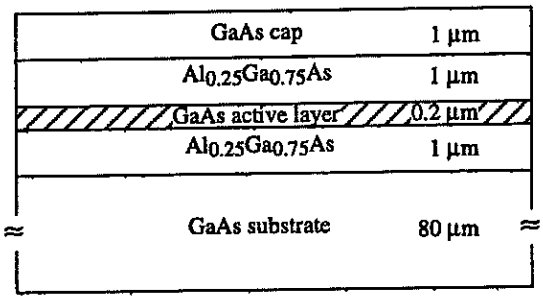

Fig. 2. The cross-section of a typical (AlGa)As laser diode.

such that

$$\sigma_s=\frac{2(3z+2t_s)}{t_s^2}\sum_{i=1}^{n}E_it_i(\alpha_i-\alpha_s)\Delta T \quad (\text{for } -t_s\le z\le 0) \tag{20}$$

$$\sigma_i=E_i(\alpha_s-\alpha_i)\Delta T \quad (\text{for } i=1 \text{ to } n) \tag{21}$$

or

$$\sigma_s=\frac{E_s(3z+2t_s)}{3r} \quad (\text{for } -t_s\le z\le 0) \tag{22}$$

$$\sigma_i=-\frac{E_st_s^2}{6t_ir_i} \quad (\text{for } i=1 \text{ to } n) \tag{23}$$

Eqs. (20)–(23) are equivalent to the approximate solutions derived by Townsend et al. [13]. While the stress in the substrate is related to the resultant curvature, $1/r$, the stress in each film layer is related to its curvature component, $1/r_i$, and is independent of the existence of other film layers [see Eq. (21)]. Also, from Eq. (20), the neutral axis is located at 2/3 of the substrate thickness underneath the film/substrate interface which has also been concluded elsewhere [14,15].

3. Results

The layer thickness in semiconductor devices is usually in the micron or submicron dimensions, and direct measurements of stresses within multilayers are difficult. The bending beam method based on the measured curvature, layer thickness, and elastic properties of the substrate [e.g. see Eqs. (22) and (23)] has often been used to estimate residual stresses in multilayer systems [5,16–19]. The analysis for thermal stresses in elastic multilayers derived by Olsen and Ettenberg [5], in which a constant Young's modulus throughout the system was assumed, has been frequently quoted [20–23]. The thermal stress distribution in (AlGa)As double-heterojunction laser diodes has also been calculated by Olsen and Ettenberg. In the lacking of direct stress measurements for multilayers, the analysis and calculated results for laser diodes by Olsen and Ettenberg are hence chosen for comparison in the present study,

A typical cross-section of the diode is shown in Fig. 2, which consists of an 80 μm GaAs substrate, a 0.2 μm active GaAs layer sandwiched between two 1 μm $Al_{0.25}Ga_{0.75}As$ confining layers, and a 1 μm GaAs cap [5]. The material properties of GaAs and AlAs have been reported: $E_{GaAs}=100$ GPa [5], $E_{AlAs}=83.5$ GPa [24], $\alpha_{GaAs}=6.86\times10^{-6}/°C$ [4], and $\alpha_{AlAs}=5.2\times10^{-6}/°C$ [25]. Also, both Young's modulus and CTE of $Al_xGa_{1-x}As$ were found to obey Vegard's rule, such that [24]

$$E_{Al_xGa_{1-x}As}=xE_{AlAs}+(1-x)E_{GaAs} \tag{24}$$

$$\alpha_{Al_xGa_{1-x}As}=x\alpha_{AlAs}+(1-x)\alpha_{GaAs} \tag{25}$$

Using Eqs. (24) and (25), the material properties of $Al_{0.25}Ga_{0.75}As$ can be obtained accordingly. It has been reported that the system is free of growth stresses because no lattice mismatch exists during growth [5,25]. Residual stresses in the above system hence result purely from the thermal mismatch and have been calculated by Olsen and Ettenberg using $\Delta T=-758$ °C; however, Young's modulus of 100 GPa was assumed throughout the system because their analytical solution was derived based on a constant E. The present analysis considers different elastic constants for each layer.

If $E=100$ GPa is assumed throughout the system in the present calculations, Olsen and Ettenberg's results can all be recovered which validates both Olsen and Ettenberg's analysis and the present analysis. Considering different elastic constants between layers, the calculated uniform strain component, c, and the total strain, ε, in the system are shown in Fig. 3. The bending strain component is the difference between ε and c. The location of the bending axis can be obtained from Eq. (8), such that $t_b=-38$ μm, which is slightly above the centreline of the substrate (at $z=-40$ μm) and can also be seen in Fig. 3. The thermal stress distributions in the substrate and film layers are shown in Fig. 4a,b, respec-

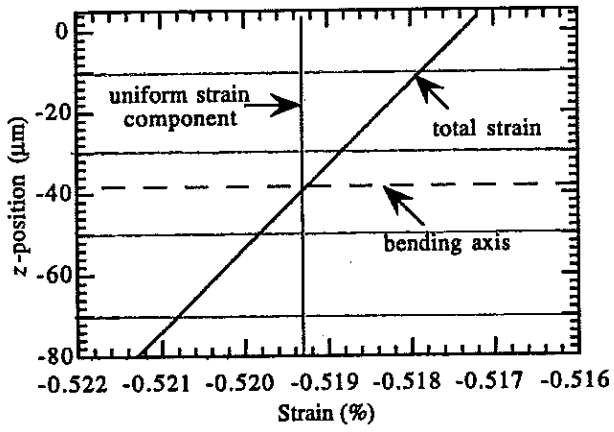

Fig. 3. The calculated uniform strain component, c, and total strain, ε, in (AlGa)As laser diodes showing the location of the bending axis.

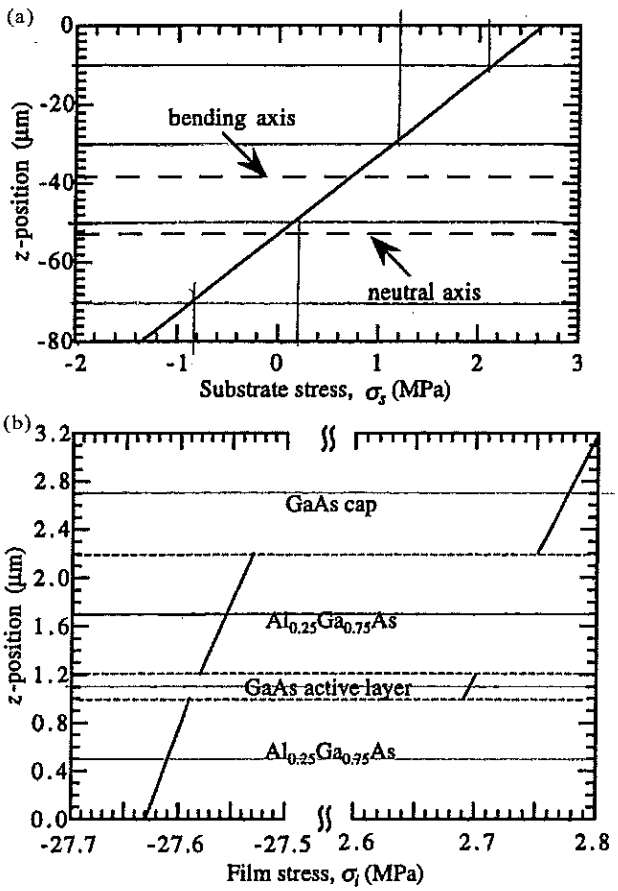

Fig. 4. Thermal stress distributions in (a) the substrate showing locations of the bending axis and the neutral axis, and (b) the film layers in (AlGa)As laser diodes.

tively. In the substrate, the top is subjected to tension and the bottom is subjected to compression. The location of the neutral axis can be obtained by finding the location with zero stress in this system, and it is located at $z=-53$ μm (which is slightly above $z=-2t_s/3$). In the film layers, the $Al_{0.25}Ga_{0.75}As$ confining layers are subjected to compression and the GaAs active layer and cap are subjected to tension because $Al_{0.25}Ga_{0.75}As$ has a lower CTE than GaAs.

To examine the accuracy of the zero-order and the first-order approximations, stress calculations are performed on (AlGa)As laser diodes to elucidate the essential trends. Comparisons of thermal stress distributions in the substrate and $Al_{0.25}Ga_{0.75}As$ and GaAs film layers are shown in Fig. 5a,b,c, respectively. It should be noted that the stress distributions in film layers are given by the exact closed-form solution, but only the average stress in each film layer can be obtained based on the zero-order and the first-order approximations (see Fig. 5b,c). While the superiority of the first-order approximation to the zero-order approximation is not obvious in the substrate (see Fig. 5a), it can be clearly seen in the film layers (Fig. 5b,c). Specifically, thermal stresses in GaAs film layers are always zero based on the zero-order approximation (Fig. 5c). This is because the thermal stress in a film layer is not influenced by the presence of other film layers in the zero-order approximation [see Eq. (21)] and the GaAs film layers have the same CTE as the GaAs substrate.

Degradation of (AlGa)As laser diodes is a major concern in applications, and studies have revealed that this degradation was caused mainly by crystalline defects created by tensile thermal stresses in the active layer. It has also been found that addition of a few percents of Al or P to the GaAs active layer to form $Al_xGa_{1-x}As$ can significantly increase the diodes' operating life [26,27]. Using Vegard's rule for the material properties of $Al_xGa_{1-x}As$, the predicted average thermal stress in the doped active layer as a function of Al contents is shown in Fig. 6. The stress in the doped active layer decreases linearly with increasing Al contents. The stress is zero when $x=2\%$ and becomes compressive for $x>2\%$.

Because constant Young's modulus throughout multilayer systems has been assumed in existing closed-form solutions [4,5,8], it is fruitful to discuss the adequacy of this assumption in the analysis. It can readily be seen from the zero-order approximation that the thermal stress in an individual film layer is linearly proportional to its Young's modulus [see Eq. (21)]. Hence, the error due to the assumption of a constant Young's modulus is expected to scale with the actual difference in Young's modulus between the substrate and film layers. To examine this error explicitly, Young's modulus of the $Al_{0.25}Ga_{0.75}As$ confining layer is varied arbitrarily while other material properties in the system remain fixed. The average thermal stress in the $Al_{0.25}Ga_{0.75}As$ layer immediately adjacent to the substrate is plotted as a function of its Young's modulus in Fig. 7. An almost linear variation of the thermal stress with Young's modulus can be seen because the film layer is relatively thin compared to the substrate.

4. Conclusions

Residual thermal stresses in multilayer systems are of interest because they influence the functionality and reliability of multilayer systems. To analyse these thermal stresses, the compatibility condition at interfaces between layers needs to be satisfied in existing analytical models [4–9]. As a result, both the number of unknowns to be solved for and the number of boundary conditions to be satisfied increase with the number of layers in the system, and closed-form solutions have often been obtained by assuming a constant elastic modulus in the system. In the present analysis, the strain distribution in the system is decomposed into a uniform strain component and a bending strain component based on the

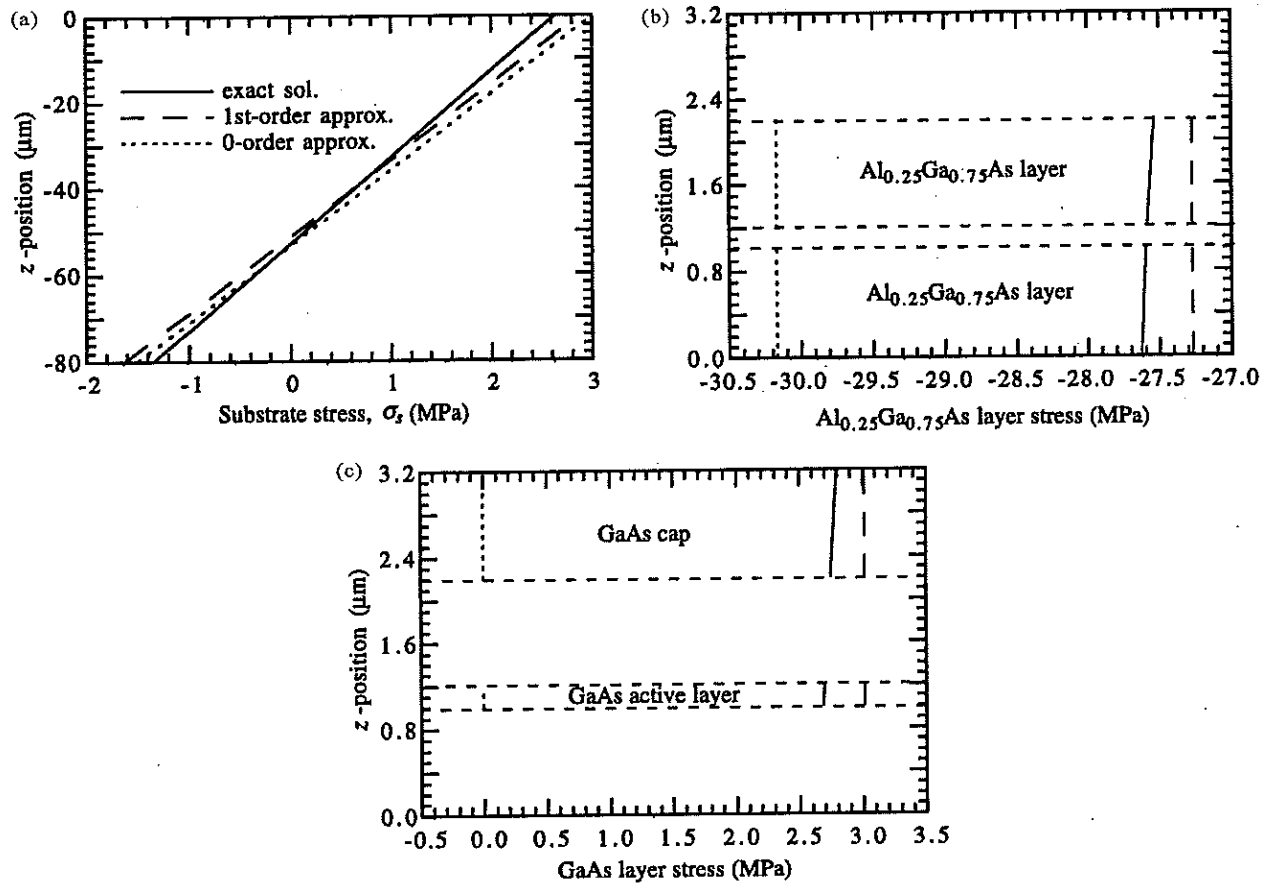

Fig. 5. Comparison between the exact solution, first-order approximation, and zero-order approximation for the stress distributions in (a) the substrate, (b) the $Al_{0.25}Ga_{0.75}As$ confining layers, and (c) the GaAs active layer and cap in (AlGa)As laser diodes. (——, exact solution; – – –, first order approximation; -----, zero-order approximation).

analytical logic of the problem (Fig. 1). Using the present approach, the compatibility condition between layers is automatically satisfied and there are always only three unknowns and three boundary conditions regardless of the number of layers in the system. In this case, a closed-form solution considering different elastic moduli for each layer can be neatly formulated. The present solution can be applied to any elastic multilayer

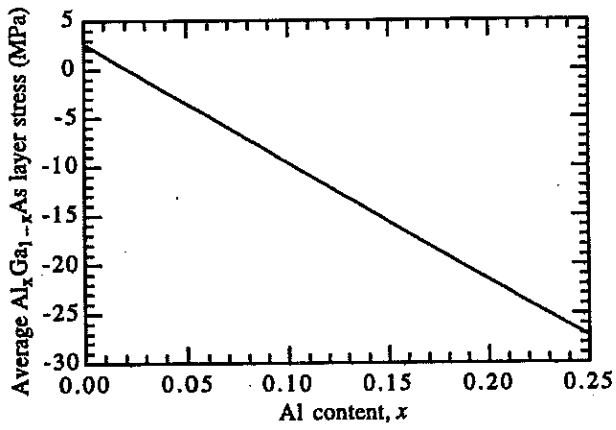

Fig. 6. The average thermal stress in the $Al_xGa_{1-x}As$ active layer as a function of the Al content, x, in (AlGa)As laser diodes.

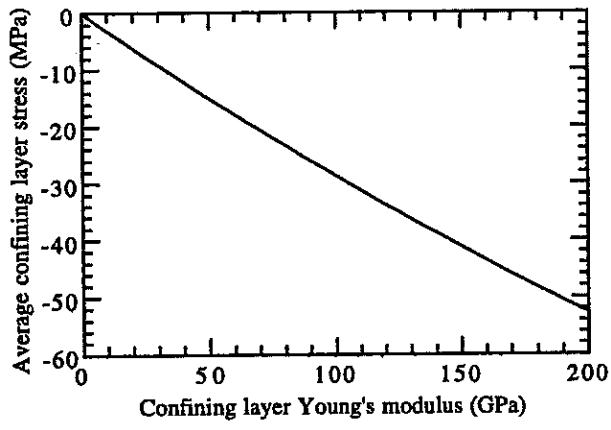

Fig. 7. The average thermal stress in the $Al_{0.25}Ga_{0.75}As$ layer immediately adjacent to the substrate as a function of its Young's modulus.

system. However, because of the difficulties in direct measurements of stresses within multilayers, the bending beam method is often used to calculate stresses in film layers based on the measured curvature. To the best of the author's knowledge, there are no direct stress measurements in multilayers to compare with. The present results are calculated for thermal stresses in five-layer (AlGa)As laser diodes, which have been frequently quoted, to elucidate the essential trends. Based on the exact closed-form solution, the first-order [Eqs. (16)–(19)] and the zero-order approximations [Eqs. (20)–(23)] can also be obtained. When the zero-order approximation is used, the thermal stress in each film layer is determined by the thermal mismatch between the substrate and that film layer and is independent of the existence of other film layers. The first-order approximation shows that the thermal stress in each film layer is influenced by the presence of other film layers. The accuracy of the first-order and the zero-order approximations can be observed in Fig. 5b,c. Also, the error in the predicted thermal stresses in film layers due to the assumption of a constant Young's modulus is expected to scale with the actual difference in Young's modulus between the substrate and film layers.

Acknowledgments

The author thanks Drs P.F. Becher, T.R. Watkins, R.D. Carneim, and M.J. Lance for useful comments. This research was sponsored by US Department of Energy, Division of Materials Sciences and Engineering, Office of Basic Energy under contract DE-AC05-00OR22725 with UT-Battelle.

References

[1] S.M. Hu, J. Appl. Phys. 70 (1991) R53.
[2] R.O.E. Vijgen, J.H. Dautzenberg, Thin Solid Films 270 (1995) 264.
[3] M.D. Tran, J. Poublan, J.H. Dautzenberg, Thin Solid Films 308–309 (1997) 310.
[4] R.H. Saul, J. Appl. Phys 40 (1969) 3273.
[5] G.H. Olsen, M. Ettenberg, J. Appl. Phys. 48 (1977) 2543.
[6] H.C. Liu, S.P. Murarka, J. Appl. Phys. 72 (1992) 3458.
[7] K. Nakajima, J. Appl. Phys. 72 (1992) 5213.
[8] V. Teixeira, Thin Solid Films 392 (2001) 276.
[9] V. Teixeira, Vacuum 64 (2002) 393.
[10] C.H. Hsueh, A.G. Evans, J. Am. Ceram. Soc. 68 (1985) 241.
[11] S. Timoshenko, J. Opt. Soc. 11 (1925) 233.
[12] J.M. Gere, S.P. Timoshenko, Mechanics of Materials, Chapman and Hall Inc, London, 1991.
[13] P.H. Townsend, D.M. Barnett, T.A. Brunner, J. Appl. Phys. 62 (1987) 4438.
[14] G.G. Stoney, Proc. R. Soc. Lond. 82 (1909) 172.
[15] J. Woltersdorf, E. Pippel, Thin Solid Films 116 (1984) 77.
[16] S. Cattarin, F. Decker, D. Dini, B. Margesin, J. Electroanal. Chem. 474 (1999) 182.
[17] J. Smolik, K. Zdunek, Surf. Coating Technol. 116–119 (1999) 398.
[18] A. Atkinson, A. Selcuk, Acta Mater. 47 (1999) 867.
[19] Y. Kim, S.H. Choo, Thin Solid Films 394 (2001) 284.
[20] H. Holloway, J. Appl. Phys. 75 (1994) 2297.
[21] T. Kozawa, T. Kachi, H. Kano, H. Nagase, N. Koide, K. Manabe, J. Appl. Phys. 77 (1995) 4389.
[22] N. Burle, B. Pichaud, N. Guelton, R.G. Saint-Jacques, Thin Solid Film 260 (1995) 65.
[23] C.H. Chen, N. Wakiya, K. Shinozaki, N. Mizutani, J. Phys. D Appl. Phys. 35 (2002) 151.
[24] S. Adachi, J. Appl. Phys. 58 (1985) R1.
[25] M. Ettenberg, R.J. Paff, J. Appl. Phys. 41 (1970) 3926.
[26] Y. Nannichi, I. Hayashi, J. Cryst. Growth 27 (1974) 126.
[27] M. Ettenberg, H. Kressel, H.F. Lockwood, Appl. Phys. Lett. 25 (1974) 82.

Residual Stresses in Metal/Ceramic Bonded Strips